

Excited state electronic properties of the [(phen)(OC)₃Re^I(NC)Ru^{II}(bpy)₂(CN)]PF₆ and [(phen)(OC)₃Re^I(CN)Ru^{II}(bpy)₂(CN)]PF₆ linkage isomers †

David W. Thompson,^{*a} Jon R. Schoonover,^b Thomas J. Meyer,^a Roberto Argazzi^c and Carlo Alberto Bignozzi^{*c}

^a Department of Chemistry, CB#3290, University of North Carolina, Chapel Hill, North Carolina 27599-3290, USA

^b Department of Chemistry, Los Alamos National Laboratory, Los Alamos, New Mexico 87545, USA

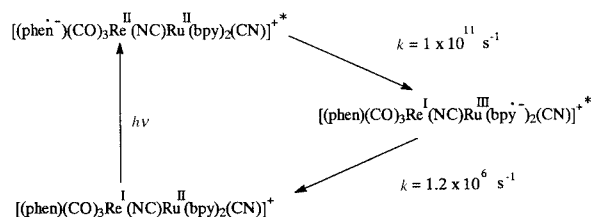
^c Dipartimento di Chimica, Centro di Studio su Fotoreattività e Catalisi CNR, Università di Ferrara, 44100, Ferrara, Italy

Received 19th July 1999, Accepted 15th September 1999

The results of temperature dependent emission lifetimes, emission spectral fitting and excited state transient absorption spectroscopy of the two hetero-dinuclear [(phen)(OC)₃Re^I(CN)Ru^{II}(bpy)₂(CN)]⁺ and [(phen)(OC)₃Re^I(NC)Ru^{II}(bpy)₂(CN)]⁺ linkage isomers (abbreviated Re–CN–Ru and Re–NC–Ru) have been examined. In both dinuclear species efficient intramolecular Re*→Ru energy transfer occurs, leading to population of emitting d_π(Ru)–π*(bpy), ³MLCT states. The temperature dependent emission data suggest that the barrier for the MLCT–dd surface crossing is smaller in magnitude when the “[phen)(OC)₃Re(NC)]” moiety is bound to the Ru(bpy)₂(CN) emitting unit. This is interpreted as the result of its enhanced ability to backbond from Ru^{II} which increases the energy of the MLCT relative to the dd states.

Introduction

The interest in the chemistry and photophysics of cyano-bridged polynuclear cations based on polypyridyl metal units stems from the observation that synthetic control of the binding mode of cyanide allows for the control of vectorial energy transfer.¹ It has recently been demonstrated that polynuclear complexes of the type [(phen)(OC)₃Re^ICN[Ru^{II}(bpy)₂CN]_nRu^{II}(bpy)₂(CN)]⁽ⁿ⁺¹⁾⁺ (where *n* = 0, 1, 2, 3) in which every Ru^{II} is bonded to one carbon and one nitrogen end of bridging cyanide are capable of supporting long-range energy transfer to the terminal Ru.² Ultrafast time-resolved infrared (TRIR) spectroscopy has been applied to the study of excited state dynamics in [(phen)(OC)₃Re^I(NC)Ru^{II}(bpy)₂(CN)]⁺ indicating that Re^I → phen excitation is followed by rapid cross bridge (5–10 ps) intramolecular energy transfer to Ru^{II}(bpy), Scheme 1.³



Scheme 1

Excited state localization in this class of polynuclear complexes has been established by application of conventional photophysical studies and, more recently, by time-resolved

resonance Raman and infrared spectroscopic methods.⁴ The spectroscopic results clearly indicated that in quasi-symmetrical dinuclear complexes of the type [(bpy)₂Ru^{II}(CN)Ru^{II}(bpy)₂(CN)]⁺ energy transfer between the MLCT states localized on the two ruthenium moieties is driven by the redox asymmetry caused by the bridge.⁵

The bridging cyanide has two positional isomers, M(CN)M' vs. M(NC)M'. The effect of the co-ordination mode of the cyano-bridge on the electrochemical and spectroscopic properties of the bridged metal ions has been demonstrated.⁵ This influence is consistent with the qualitative view that C-bonded cyanide acts as typical strong-field π-acid ligand. In contrast, the N-bonded cyanide behaves like a medium-field, mainly σ-donor ligand. How the binding mode can affect the excited state properties of a ruthenium(II) polypyridine fragment can be established by considering the photophysical properties of two linkage isomeric species. The results from temperature dependent emission lifetimes, emission spectral fitting and excited state transient absorption spectroscopy of the two hetero-dinuclear [(phen)(OC)₃Re^I(CN)Ru^{II}(bpy)₂(CN)]⁺ and [(phen)(OC)₃Re^I(NC)Ru^{II}(bpy)₂(CN)]⁺ linkage isomers (abbreviated Re–CN–Ru and Re–NC–Ru throughout) have been critically examined and form the basis of the present manuscript.

Experimental

Preparations

[(phen)(OC)₃Re^I(CN)Ru^{II}(bpy)₂(CN)]PF₆. Sodium azide (0.0171 g, 0.79 mmol) dissolved in 2 mL of methanol was added slowly with stirring over a period of 15 min to a suspension of [Ru(bpy)₂(NO)(CN)]PF₆ (0.2 g, 0.26 mmol) in methanol (20 mL). The purple-brown solution was stirred at room temperature for 30 min followed by the addition of [Re^I(CO)₃(phen)(CN)] (0.25 g, 0.52 mmol) in methanol (150 mL). The solution

† Supplementary data available: temperature-dependent relative emission intensities and lifetimes. For direct electronic access see <http://www.rsc.org/suppdata/dt/1999/3729/>, otherwise available from BLDSC (no. SUP 57646, 6 pp.) or the RSC Library. See Instructions for Authors, 1999, Issue 1 (<http://www.rsc.org/dalton>).

was refluxed for 6 h and evaporated to dryness. The resulting solid was stirred in acetonitrile and the unchanged $[\text{Re}^{\text{I}}(\text{CO})_3(\text{phen})(\text{CN})]$ filtered off. The solution was loaded on a silica column and elution was performed first with CH_2Cl_2 – CH_3CN (1:1 v/v) to collect $[\text{Re}^{\text{I}}(\text{CO})_3(\text{phen})(\text{CN})]$ and then with methanol to collect the brown Re–CN–Ru dimer. The methanol solution was evaporated and the solid dried under vacuum. Calc. for $[(\text{phen})(\text{OC})_3\text{Re}^{\text{I}}(\text{CN})\text{Ru}^{\text{II}}(\text{bpy})_2(\text{CN})]\text{PF}_6$: C, 41.89; H, 2.28; N, 2.28. Found: C, 41.70; H, 2.18; N, 2.32%.

$[(\text{phen})(\text{OC})_3\text{Re}^{\text{I}}(\text{NC})\text{Ru}^{\text{II}}(\text{bpy})_2(\text{CN})]\text{PF}_6$. The $[\text{Re}^{\text{I}}(\text{CO})_3(\text{phen})\text{Cl}]$ (0.0514 g, 0.106 mmol) and $[\text{Ru}(\text{bpy})_2(\text{CN})_2]$ complexes (0.101 g, 0.217 mmol) were dissolved in boiling methanol (40 mL) under argon. The solution was refluxed for 5 h and evaporated to dryness. The resulting solid was stirred in cold water and the unchanged $[\text{Ru}(\text{bpy})_2(\text{CN})_2]$ complex filtered off. The crude product was precipitated with addition of solid NH_4PF_6 . The precipitate was dissolved in methanol and chromatographed on silica gel using methanol as an eluent. Red-orange $[\text{Ru}(\text{bpy})_2(\text{CN})_2]$ was collected first followed by an orange fraction containing the binuclear Re–NC–Ru complex. The second fraction was rotary evaporated to dryness. The elemental analysis was identical to that of the linkage isomer. FAB Mass spectra for both $\text{Re}(\text{CN})_x\text{Ru}$ (where $(\text{CN})_x$ designates both isomers) have been reported previously.⁶

In situ generation of oxidized complexes

Acetonitrile solutions of the oxidized species $[(\text{phen})(\text{OC})_3\text{Re}^{\text{I}}(\text{CN})\text{Ru}^{\text{III}}(\text{bpy})_2(\text{CN})]^{2+}$ were prepared by titration with $[\text{NH}_4]_2[\text{Ce}(\text{NO}_3)_6]$. Solutions containing $\text{Re}^{\text{I}}\text{–CN–Ru}^{\text{III}}$ were stable for spectroscopic characterization experiments. Oxidation of Re–NC–Ru led to decomposition of the complex.

Ground and excited state measurements

UV-Visible spectra were recorded by using a Hewlett Packard model 8451A Diode Array spectrophotometer or with a Kontron Uvikon 860 spectrophotometer. Cyclic voltammetric measurements were performed in acetonitrile solutions in the presence of 0.1 M tetrabutylammonium hexafluorophosphate, a platinum working electrode, and a SCE reference electrode with previously described instrumentation.⁶

Emission and emission spectral fitting

Samples for lifetime and emission experiments were prepared as optically dilute solutions ($A < 0.2$ at the λ_{max} in a 1.00 cm cell) in CH_3CN or EtOH–MeOH (4:1 v/v), freeze–pump–thaw degassed for at least three cycles and sealed under vacuum.

Emission spectra were measured on a Perkin-Elmer MPF 44E spectrofluorimeter equipped with a Hamamatsu R 928 tube or with a Spex Fluorolog F212 photon counting spectrofluorimeter equipped with either a R 928 or R 666-10 red sensitive Hamamatsu phototube. All reported spectra were corrected for instrument response.

Relative emission quantum yields were measured in deoxygenated acetonitrile and ethanol–methanol (4:1 v/v) solutions at 25 °C with $\text{Re}(\text{CN})_x\text{Ru}$ samples where $A < 0.2$ at the λ_{exc} , and compared those off to a standard sample of $[\text{Ru}(\text{bpy})_3][\text{PF}_6]_2$ in acetonitrile solutions for which $\Phi_{\text{std}} = 0.062$ at $\lambda_{\text{exc}} = 460$ nm.⁷ Relative emission quantum yields were calculated using eqn. (1), where A is the solution absorbance, I the

$$\varphi_{\text{em}} = \varphi_{\text{std}} \left(\frac{A_{\text{std}}}{A_o} \right) \left(\frac{I_o}{I_{\text{std}}} \right) \left(\frac{n_o}{n_{\text{std}}} \right)^2 \quad (1)$$

emission intensity, n the index of refraction of the solvent and the subscripts o and std refer to the unknown and standard, respectively.

For the purposes of emission spectral fitting, emission spectra were normalized and the emission abscissa converted into an abscissa linear in energy by the method of Parker and Rees.⁸ The emission spectral procedure used a modification of the previously described procedures and protocols employing a single mode Franck–Condon analysis, eqn. (2), which

$$I(\bar{\nu}) = \sum_{v_M=0}^5 \left(\frac{E_o - v_M \hbar \omega_M}{E_o} \right)^3 \left(\frac{S_M^{v_M}}{v_M!} \right) \exp \left[-4 \ln(2) \left(\frac{\bar{\nu} - E_o + v_M \hbar \omega_M}{\Delta \bar{\nu}_{0,1/2}} \right)^2 \right] \quad (2)$$

adequately fit the data at 77 and 298 K.⁹ In eqn. (2), $I(\bar{\nu})$ is the emitted light intensity at energy (in cm^{-1}) relative to the maximum in the emission profile, v_M the vibrational quantum number for the medium frequency acceptor mode of quantum spacing $\hbar \omega_M$ and the electron-vibrational coupling constant S_M . The quantity E_o is the energy gap (in cm^{-1}) between the excited and ground states for the $v'_M = 0 \rightarrow v_M = 0$ transition; S_M is related to the difference in the equilibrium displacements between the excited and ground states (Δq_M) and the reduced mass M by eqn. (3). The term $\Delta \bar{\nu}_{0,1/2}$ is the full width

$$S_M = \frac{1}{2} \left(\frac{M \omega}{\hbar} \right) (\Delta q_M)^2 \quad (3)$$

at half-maximum (fwhm) for the vibronic components. It includes contributions from both the solvent reorganization energy (λ_o) and the low frequency acceptor modes treated classically.

Time resolved emission

Emission lifetimes were measured with a J&K System 2000 ruby laser (frequency doubled, pulse half-width of 25 ns) or with 460 nm excitation using a PRA LN102 dye laser pumped by a LN100 N_2 laser. The excitation beam was passed through a collection of lenses and defocused onto the sample cell. Scattered light was removed by a dichromate cut-off filter. Emission decay was monitored at right angles with a PRA B204-3 2.5 monochromator and a Hamamatsu R 928 water cooled photomultiplier tube. Either a LeCroy 7200 or 9360 digitizing oscilloscope was used to collect the time dependent emission traces. IBM PC or Gateway 2000 microcomputers were employed for data analysis. Emission decays were independent of monitoring wavelength, and could be satisfactorily fit by a single exponential decay function. Reported lifetimes are the average of 150–200 decay traces. Emission lifetimes at 77 K were measured by using a liquid N_2 finger dewar or at variable temperature (120–270 K) by using a Janis Model NDT-6 Cryostat coupled to a Lakeshore DRC-84C temperature controller. Temperature control for lifetime data from 274 to 303 K was measured with a Neslab Instrument Endocal RTE-110 water circulator coupled to a close fitting brass block. The temperature was read with a thermocouple directly attached to the cell. In the transient emission experiments a PRA LN1000 pulsed nitrogen laser was used as an excitation source at 337 nm coupled to a PRA grating LN102/1000 tunable dye head.

Transient absorption spectroscopy

Transient absorption (TA) experiments were conducted as previously described.² Acetonitrile solutions of the dinuclear complexes in the concentration range 1×10^{-4} – 1.5×10^{-4} M were excited at 347 nm with a ruby laser delivering 25 ns (half-width) pulses. Transient absorbance difference spectra were converted into molar absorptivity changes by standardization against absorbance-matched solutions of benzophenone in benzene.

Table 1 Photophysical properties in 4:1 EtOH–MeOH at 77 and 298 K

Complex	$\lambda_{\text{max}}^{\text{Abs}}/\text{nm}$	$\lambda_{\text{em}}/\text{nm}$	298 K		77 K	
			Φ_{em}	τ/ns	$\lambda_{\text{em}}/\text{nm}$	$\tau/\mu\text{s}$
[Ru(bpy) ₃][PF ₆] ₂	450	630 ^a	0.062 ^a	910	582	5.1
[Ru(bpy) ₂ (CN) ₂]	458	653 ^b	0.038 ^c	390	592	3.96
[(phen)(OC) ₃ Re(NC)Ru(bpy) ₂ (CN)] ⁺	450	618		622	568, 614	5.84
[(phen)(OC) ₃ Re(CN)Ru(bpy) ₂ (CN)] ⁺	472	672	0.019	429	598, 644	4.01

^a Ref. 7. ^b Ref. 9. ^c In MeOH solution.¹⁰

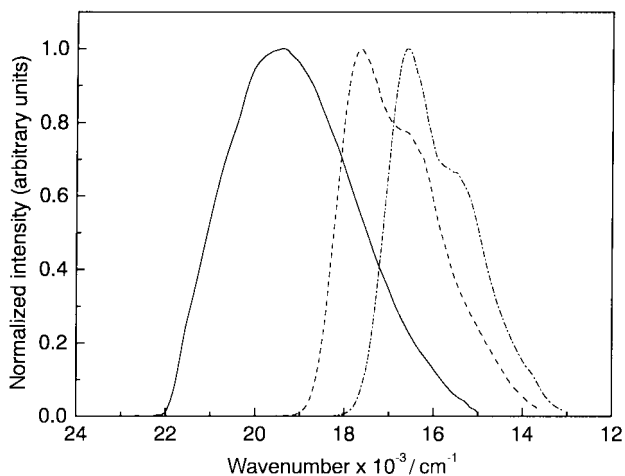


Fig. 1 77 K Corrected emission spectra of [Re^I(CO)₃(phen)(CN)] (—), [(phen)(OC)₃Re^I(NC)Ru^{II}(bpy)₂(CN)]⁺ (---) and [(phen)(OC)₃Re^I(CN)Ru^{II}(bpy)₂(CN)]⁺ (-.-.) in EtOH–MeOH (4:1 v/v).

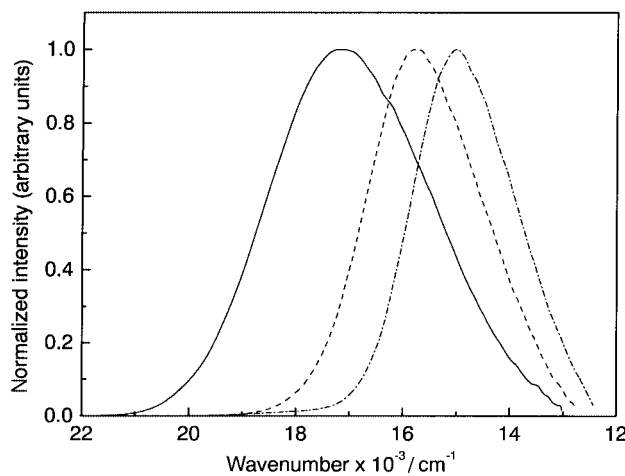


Fig. 2 298 K Corrected emission spectra in CH₃CN. Key as in Fig. 1.

Results

Electrochemistry

Redox potentials for Re–CN–Ru and Re–NC–Ru were measured by cyclic voltammetry in CH₃CN solution ([[(C₄H₉)₄N]-PF₆ = 0.1 M) vs. SCE. The linkage isomers exhibit two oxidation waves which can be assigned to oxidation of the ruthenium(II) and rhenium(I) centers from comparison with the electrochemistry of [Ru(bpy)₂(CN)₂], where $E_{1/2}(\text{Ru}^{\text{III/II}}) = +0.86$ V, and [Re(CO)₃(phen)(CN)], where $E_p(\text{Re}^{\text{III}}) = +1.58$ V. Halfwave potentials, $E_{1/2}$, for the Ru^{III/II} redox couples are +0.94 and +1.10 V for Re–CN–Ru and Re–NC–Ru respectively. Oxidation of Re^I to Re^{II} was not reversible. For this process, anodic peak potentials, E_p , of +1.78 and +1.74 V were estimated at scan rates of 100 mV s⁻¹ for Re–CN–Ru and Re–NC–Ru, respectively.

Excited state properties

Absorption maxima, emission maxima and emission lifetimes for Re–CN–Ru and Re–NC–Ru in EtOH–MeOH (4:1 v/v) are given in Table 1 with comparative literature data for [Ru(bpy)₃]²⁺ and [Ru(bpy)₂(CN)₂]. Steady-state emission spectra for Re–CN–Ru and Re–NC–Ru at 77 K in EtOH–MeOH (4:1 v/v) and 298 K in CH₃CN are shown in Figs. 1 and 2 respectively.

The low energy visible absorption bands for the linkage isomers arise from Ru^{II}→bpy MLCT transitions. These bands are solvent dependent with the MLCT maxima varying qualitatively as maxima for [Ru(bpy)₂(CN)₂].¹¹ In EtOH–MeOH (4:1 v/v), the MLCT energies follow the descending order: Re–NC–Ru > [Ru(bpy)₂(CN)₂] > Re–CN–Ru.

The linkage isomers are long lived intense emitters in fluid solution at room temperature. Previous studies,^{1,12} have shown that E_{em} for [(phen)(OC)₃Re^I(CN)Ru^{II}(bpy)₂(CN)]⁺ varies linearly with the acceptor number of the solvent, a trend which is observed for [Ru(bpy)₂(CN)₂] and other cyano complexes as

well.¹³ The E_{em} values in EtOH–MeOH (4:1 v/v) follow the order: Re–NC–Ru > [Ru(bpy)₂(CN)₂] > Re–CN–Ru, which is the ordering of the MLCT band energies. The increases in E_{em} in rigid alcoholic glass at 77 K relative to fluid solution are common (Table 1) and arise because the surrounding solvent dipoles are frozen in ground state orientations.¹³

Emission spectral fitting

Emission spectral data at 77 and 298 K are given in Table 1, emission spectral fitting parameters in Table 2 with data for [Ru(bpy)₃]²⁺ for comparison. The emission spectra are convolutions of vibronic contributions from a series of medium frequency (bpy) ring stretching modes and a series of low frequency modes, which include (M–L) metal–ligand stretching vibrations.⁹ The S_M values derived by emission spectral fitting are the sum, $S_M = \sum_j S_j$, and the weighted sums $\hbar\omega_M = \sum_j S_j \hbar\omega_j / \sum_j S_j$ of the coupled medium frequency vibrations. The solvent and low frequency vibrations treated classically are included in $\Delta\tilde{\nu}_{0,1/2}$. This parameter is related to the solvent reorganizational energy (λ_o) and the reorganizational energy from the low frequency modes treated classically ($\lambda_{i,L}$) by eqn. (4).

$$(\Delta\tilde{\nu}_{0,1/2})^2 = (16\ln(2)k_{\text{B}}T)(\lambda_o + \lambda_{i,L}) \quad (4)$$

Temperature dependent emission lifetimes

The results of temperature dependent lifetime studies on Re–NC–Ru and Re–CN–Ru in 4:1 (v/v) EtOH–MeOH are compared with those of [Ru(bpy)₂(CN)₂] and [Ru(bpy)₃][PF₆]₂ in Table 3 and plots of the excited state lifetimes as a function of temperature are shown in Figs. 3 and 4.

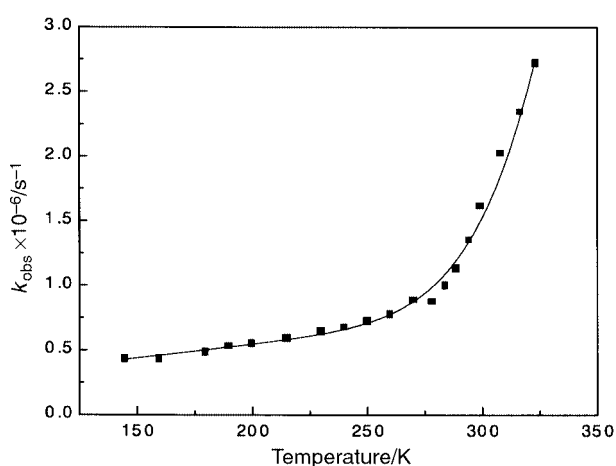
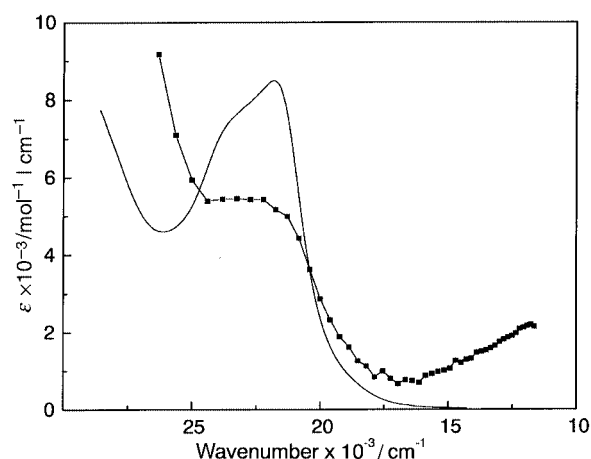
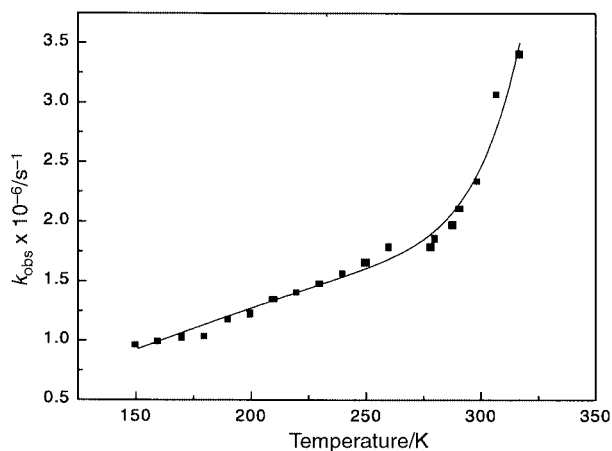
The decay kinetics for Re–CN–Ru in 4:1 (v/v) EtOH–MeOH is non-exponential and complex in the glass to fluid transition region (110–140 K) because of kinetic coupling between medium relaxation and excited state decay.^{15,16} The kinetics for excited state decay was found to be exponential in fluid solution. Temperature dependent luminescence decays in the $T = 150$ to 310 K regime were fit using eqn. (5). Individual life-

Table 2 Emission spectral fitting parameters in 4:1 EtOH–MeOH at 77 and 298 K

Complex	<i>T</i> /K	<i>E</i> _{em} /cm ⁻¹	$\hbar\omega_M$ /cm ⁻¹	<i>E</i> ₀ /cm ⁻¹	<i>S</i> _M	$\Delta\nu_{0,1/2}$ /cm ⁻¹	ln[<i>F</i> (calc.)] ^a
[Ru(bpy) ₃][PF ₆] ₂	77	17180	1350	17090	1.12	976	-20.45
	298	15873	1350	16300	1.10	1749	-18.63
[(phen)(OC) ₃ Re(NC)Ru(bpy) ₂ (CN)] ⁺	77	17606	1340	17491	1.12	1122	-21.31
	298	16180	1340	16350	0.93	1750	-20.60
[(phen)(OC) ₃ Re(CN)Ru(bpy) ₂ (CN)] ⁺	77	16720	1320	16693	1.14	1152	-20.07
	298	14880	1320	15237	0.84	1939	-19.71

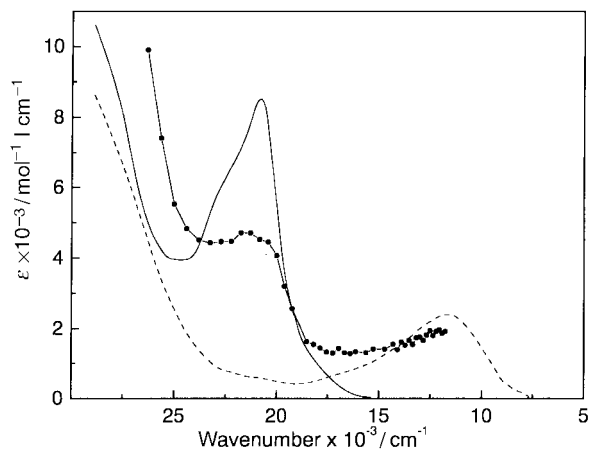
^a Ref. 13.**Table 3** Comparative room temperature photophysical properties and kinetic decay parameters from lifetime measurements in 4:1 EtOH–MeOH

Complex	10 ⁻⁵ <i>k</i> ₀ /s ⁻¹	<i>k</i> ₁ ⁰ /s ⁻¹	ΔE_1 /cm ⁻¹	<i>k</i> ₂ ⁰ /s ⁻¹	ΔE_2 /cm ⁻¹
[Ru(bpy) ₃][PF ₆] ₂ ^a	2.2	5.0 × 10 ⁷	69	2.0 × 10 ¹⁴	4040
[Ru(bpy) ₂ (CN) ₂] ^b	2.8	2.6 × 10 ⁷	450	3.0 × 10 ¹⁰	2400
[(phen)(OC) ₃ Re(NC)Ru(bpy) ₂ (CN)] ⁺ ^c	3.2	1.5 × 10 ⁶	264	3.0 × 10 ¹¹	2680
[(phen)(OC) ₃ Re(CN)Ru(bpy) ₂ (CN)] ⁺ ^c	4	4.1 × 10 ⁶	215	3.5 × 10 ¹³	3730

^a Ref. 14. ^b Ref. 21. ^c The data were adequately fit by a two state model using eqn. (5) (*T* = 150–300 K).**Fig. 3** Temperature dependence of lifetime for [(phen)(OC)₃Re^I(NC)Ru^{II}(bpy)₂(CN)]⁺ in EtOH–MeOH (4:1 v/v).**Fig. 5** Ground state (—) and excited state (—■—) absorption spectra of [(phen)(OC)₃Re^I(NC)Ru^{II}(bpy)₂(CN)]⁺ in acetonitrile.**Fig. 4** Temperature dependence of lifetime for [(phen)(OC)₃Re^I(CN)Ru^{II}(bpy)₂(CN)]⁺ in EtOH–MeOH (4:1 v/v)

$$[\tau(T)^{-1}] = k_{\text{obs}} = k_0 + k_1^0 \exp\left[\frac{-\Delta E_1}{k_B T}\right] + k_2^0 \exp\left[\frac{-\Delta E_2}{k_B T}\right] \quad (5)$$

times and relative emission yields are reported in SUP 57646. In eqn. (5) it is assumed that emitting states are reached with unit efficiency and $\Delta E \gg k_B T$, and $k_0 = k_r + k_{nr}$ where k_r and k_{nr} are the rate constants for radiative and non-radiative decay, respectively, from the lowest emitting MLCT state or states,¹⁵ k_0 is expected to be only slightly temperature dependent. The quan-

**Fig. 6** Ground state absorption spectra of [(phen)(OC)₃Re^I(CN)Ru^{II}(bpy)₂(CN)]⁺ (—) and [(phen)(OC)₃Re^I(CN)Ru^{III}(bpy)₂(CN)]²⁺ (---), and excited state absorption spectrum of [(phen)(OC)₃Re^I(CN)Ru^{II}(bpy)₂(CN)]⁺ (—●—) in acetonitrile.

ties, k_1^0 , k_2^0 , ΔE_1 and ΔE_2 are the pre-exponential and energy gap terms which include thermal activation and decay from higher states.

Excited state absorption spectra

Excited state absorption (ESA) spectra of Re–NC–Ru and Re–CN–Ru are reported in Figs. 5 and 6. Ground state absorp-

tion spectra of $\text{Re}^{\text{I}}\text{-CN-Ru}^{\text{II}}$ and the oxidized $\text{Re}^{\text{I}}\text{-CN-Ru}^{\text{III}}$ species are also shown. The excited state spectra are dominated by an intense absorption band in the visible region, similar to those observed for $[\text{Ru}(\text{bpy})_2(\text{CN})_2]$.² At lower energy, absorption features have contributions from metal-to-metal charge transfer transition involving Re^{I} and the excited $\text{Ru}^{\text{III}}(\text{bpy}^{\cdot-})^*$ units.

Discussion

Directional energy transfer for $[(\text{phen})(\text{OC})_3\text{Re}^{\text{I}}(\text{NC})\text{Ru}^{\text{II}}(\text{bpy})_2(\text{CN})]^+$ from the energetically higher lying Re based MCLT excited state to the lower-lying Ru based MLCT excited states has been conclusively demonstrated by a combination of transient absorption and ultra-fast and ns transient infrared measurements, Scheme 1.¹ Vectorial energy transfer also occurs in $[(\text{phen})(\text{OC})_3\text{Re}^{\text{I}}(\text{CN})\text{Ru}^{\text{II}}(\text{bpy})_2(\text{CN})]^+$, however the bonding mode of the bridging CN influences both the photophysical and photochemical properties of the “ $\text{Ru}^{\text{II}}(\text{bpy})_2(\text{CN})$ ” component. The new photophysical data acquired in this work on the Re–NC–Ru and Re–CN–Ru linkage isomers lend insight into how the mode of coordination of the bridging cyanide influences the excited state properties of the energy accepting ruthenium polypyridyl fragment.

Electronic structure

Low energy absorption and MLCT emissions in Re–NC–Ru and Re–CN–Ru are based on the $\text{Ru}(\text{bpy})$ chromophore.¹ The $\text{Re}^{\text{I}} \rightarrow \text{phen}$ excitation is followed by rapid cross-bridge energy transfer.^{1,3} The order of increasing MLCT absorption and $\text{Ru}^{\text{III}}(\text{bpy}^{\cdot-})$ emission band maxima $\text{Re-NC-Ru} > [\text{Ru}(\text{bpy})_2(\text{CN})_2] > \text{Re-CN-Ru}$ can be rationalized qualitatively on straightforward bonding arguments and the electronic character of $[(\text{phen})(\text{OC})_3\text{Re}(\text{NC})]$, CN^- , and $[(\text{phen})(\text{OC})_3\text{Re}(\text{CN})]$ “ligands”. Analysis of the visible spectra indicates a ligand π -acceptor order of $[(\text{phen})(\text{OC})_3\text{Re}(\text{NC})]$, CN^- , and $[(\text{phen})(\text{OC})_3\text{Re}(\text{CN})]$. The π -bonding abilities of CN^- are thought to be low relative to CO, for example, and only become important for low valent metals such as Ni^0 .¹⁷ In $[(\text{phen})(\text{OC})_3\text{Re}(\text{NC})]$, electron pair donation from CN^- to Re^{I} renders the metal complex/ligand more π -acidic than CN^- .¹⁸ This enhances $^d\pi\text{-}\pi^*$ back donation and increases the $^d\pi(\text{Ru}^{\text{II}})\text{-}\pi^*(\text{bpy})$ energy gap. The effect of $\text{Re}^{\text{I}}\text{-NC}$ bonding on CN^- is similar to that found in isocyanides, RNC, which are known to be good π -bonding ligands.¹⁸ Compared to CN^- , there is a red shift of the MLCT absorption and emission bands with “[$(\text{phen})(\text{OC})_3\text{Re}(\text{CN})$]” as the sixth ligand. Inspection of the electron density maps for $\text{M}(\text{CN})_6$ complexes¹⁸ suggests that the nitrogen terminus of co-ordinated CN^- in “[$(\text{phen})(\text{OC})_3\text{Re}(\text{CN})$]” would be a poorer π acceptor and give rise to a smaller $^d\pi(\text{Ru}^{\text{II}})\text{-}\pi^*(\text{bpy})$ energy gap.

As derived from the emission spectral fitting procedure, $\hbar\omega_M$ for the linkage isomers, Re–CN–Ru and Re–NC–Ru, were in the 1320 to 1350 cm^{-1} range. The near constancy of $\hbar\omega_M$ for both linkage isomers points to a common pattern of acceptor vibrations which are not significantly perturbed by the mode of coordination of the bridging CN^- group. The red shifts in E_0 for Re–NC–Ru (1141 cm^{-1}) and Re–CN–Ru (1456 cm^{-1}) in EtOH–MeOH (4:1 v/v) between 298 K fluid solution and 77 K rigid glasses are larger than found for $[\text{Ru}(\text{bpy})_3][\text{PF}_6]_2$ (790 cm^{-1}). The shifts arise because emission in the glass occurs with the dipole part of the solvent polarization frozen as it is in the ground state, while in fluid solution it relaxes to the equilibrium polarization of the excited state.¹³ The effect is magnified in the cyano complexes because of the existence of specific electron pair donor–acceptor interactions between the CN^- lone pair and the individual solvent molecules.¹¹ The decrease in S_M from the rigid glass to fluid solution is a manifestation of the

decreased energy gap, E_0 . It has been previously observed that S_M decreases linearly with E_0 for a series of polypyridyl complexes of Os^{II} and Ru^{II} .²⁰

Non-radiative decay

Excited state lifetimes for Re–CN–Ru in EtOH–MeOH (4:1 v/v) solution are temperature dependent. In other polypyridyl complexes of Ru^{II} such temperature dependences have been attributed to thermal activation and decay through low-lying dd and MLCT excited states.¹⁴ In treating the temperature dependence of excited state decay for $[\text{Ru}(\text{bpy})_2(\text{CN})_2]$, Barigelletti *et al.*²¹ found that two temperature dependent terms were required. In the limited temperature range examined we find the same, with kinetic parameters defining the exponential terms that seem reasonable.

The magnitudes of the kinetic parameters for the first exponential term (k_1^0 , ΔE_1) fall in ranges ($10^7\text{--}10^9 \text{ s}^{-1}$; 200–800 cm^{-1}) that have been attributed to thermal activation and decay from a higher lying MLCT state or states.^{14,22} Similar temperature dependent terms appear, for example, in non-radiative decay of polypyridyl complexes of Os^{II} where there are no complications from low-lying dd states. Assuming rapid kinetic interconversion between states, ΔE_1 is the MLCT–MLCT energy gap and k_1^0 is the decay rate constant. For $[\text{M}(\text{bpy})_3]^{2+}$ ($\text{M} = \text{Ru}^{\text{II}}$ or Os^{II}), $k_1^0 > k_0$ because of enhanced singlet character in the upper MLCT state.²²

The kinetic parameters for the second exponential term (k_2^0 and ΔE_2) are associated with the thermally activated MLCT–dd surface crossing. Once populated the dd states undergo rapid non-radiative decay and often competitive ligand loss photochemistry. The kinetics of decay through this pathway is complex, and different limits have been discussed.^{14,23} In one, irreversible MLCT–dd surface crossing occurs. In this limit k_2^0 is the preexponential term (typically $10^{12}\text{--}10^{14} \text{ s}^{-1}$) and ΔE_2 the energy of activation (typically 2500–4000 cm^{-1}) for the transition. In a second kinetic limit the MLCT and dd states are in kinetic equilibrium and k_2^0 is the rate constant for decay of the dd state and ΔE_2 is the energy gap between the states. In comparing k_2^0 and ΔE_2 values in Table 3, their magnitudes for $[(\text{phen})(\text{OC})_3\text{Re}^{\text{I}}(\text{CN})\text{Ru}^{\text{II}}(\text{bpy})_2(\text{CN})]^+$ and $[\text{Ru}(\text{bpy})_3]^{2+}$ suggest decay by irreversible MLCT–dd surface crossing. The data for $[\text{Ru}(\text{bpy})_2(\text{CN})_2]$ and $[(\text{phen})(\text{OC})_3\text{Re}^{\text{I}}(\text{NC})\text{Ru}^{\text{II}}(\text{bpy})_2(\text{CN})]^+$ fall in the intermediate regime.

As found earlier for $[\text{Ru}(\text{bpy})_3]^{2+}$ and $[\text{Ru}(\text{phen})_2(\text{CN})_2]$ in a series of solvents and for a series of ruthenium(II) polypyridyl complexes in the same solvent, a linear correlation exists for the series of cyano complexes between $\ln k_2^0$ and ΔE_2 .²⁴ This “Barclay Butler” plot for the ruthenium(II) polypyridyl complexes gave a linear correlation with slope = $2.9 \times 10^{-3} \text{ cm}$ and intercept = 5.1 ($R = 0.99$ for 10 data points). For the cyano complexes considered here a less well defined correlation exists with slope = $5 \times 10^{-3} \text{ cm}$ and intercept = 11.5 ($R = 0.9$). It has been argued that these correlations exist because an increase in the activation barrier is accompanied by a greater density of vibrational levels at the point of barrier crossing effectively increasing the number of reaction channels. These effects are expected to be dominated by low frequency collective dipole reorientation of the solvent as discussed previously.^{13,24} They may be amplified in the cyano series as evidenced by the larger slope in the Barclay Butler plot due to specific solute–solvent interactions involving the CN.

The temperature dependent data show that ΔE_2 for Re–CN–Ru $>$ Re–NC–Ru. If the conclusion that these two decay in different kinetic regimes is correct, the parameters cannot be directly compared. However, it can be inferred that the barrier for the MLCT–dd surface crossing is smaller in magnitude when the “[$(\text{phen})(\text{OC})_3\text{Re}(\text{NC})$]” moiety is the “ligand”. This

is the result of its enhanced π acidity so that for Ru^{II} the energy of the MLCT state increases relative to the dd state.

Acknowledgements

We are grateful to the National Science Foundation for Grant CHE-9705724 and to the Natural Science and Engineering Research Council of Canada (NSERC) for a postdoctoral fellowship to D. W. T. for portions of this work completed at the Department of Chemistry, University of North Carolina at Chapel Hill. C. A. B. acknowledges EU for financial support under Contract No. JOR3CT98-7040.

References

- 1 C. A. Bignozzi, R. Argazzi, C. G. Garcia, F. Scandola, J. R. Schoonover and T. J. Meyer, *J. Am. Chem. Soc.*, 1992, **114**, 8727.
- 2 C. A. Bignozzi, R. Argazzi, C. Chiorboli, F. Scandola, R. B. Dyer, J. R. Schoonover and T. J. Meyer, *Inorg. Chem.*, 1994, **33**, 1652.
- 3 J. R. Schoonover, K. C. Gordon, R. Argazzi, W. H. Woodruff, K. A. Peterson, C. A. Bignozzi, R. B. Dyer and T. J. Meyer, *J. Am. Chem. Soc.*, 1993, **115**, 10996.
- 4 C. A. Bignozzi, J. R. Schoonover and R. B. Dyer, *Comments Inorg. Chem.*, 1996, **18**, 77; J. R. Schoonover and G. F. Strouse, *Chem. Rev.*, 1998, **98**, 1335; J. R. Schoonover, G. F. Strouse, K. M. Omberg and R. B. Dyer, *Comments Inorg. Chem.*, 1996, **18**, 165.
- 5 C. A. Bignozzi, R. Argazzi, C. Chiorboli, S. Roffia and F. Scandola, *Coord. Chem. Rev.*, 1991, **111**, 261; K. Kalyanasundaram, M. Gratzel and Md. K. Nazeeruddin, *Inorg. Chem.*, 1992, **31**, 5243; C. A. Bignozzi, S. Roffia, C. Chiorboli, J. Davila, M. T. Indelli and F. Scandola, *Inorg. Chem.*, 1989, **28**, 4350; C. A. Bignozzi, R. Argazzi, J. R. Schoonover, K. C. Gordon, R. B. Dyer and F. Scandola, *Inorg. Chem.*, 1992, **31**, 5260.
- 6 R. Argazzi, C. A. Bignozzi, O. Bortolini and P. Traldi, *Inorg. Chem.*, 1993, **32**, 1222.
- 7 J. M. Calvert, J. V. Caspar, R. A. Binstead, T. D. Westmoreland and T. J. Meyer, *J. Am. Chem. Soc.*, 1992, **114**, 6620; S. L. Mecklenburg, B. M. Peek, J. R. Schoonover, D. G. McCafferty, B. W. Erickson and T. J. Meyer, *J. Am. Chem. Soc.*, 1993, **115**, 5479.
- 8 C. A. Parker and W. T. Rees, *Analyst (London)*, 1960, **85**, 857.
- 9 J. P. Claude, Ph.D. Thesis, University of North Carolina, Chapel Hill, 1991; P. F. Barbara, T. J. Meyer and M. A. Ratner, *J. Phys. Chem.*, 1996, **100**, 13148.
- 10 P. Belser, A. von Zelewsky, A. Juris, F. Barigelletti and V. Balzani, *Gazz. Chim. Ital.*, 1985, **115**, 723.
- 11 C. J. Timpson, C. A. Bignozzi, B. P. Sullivan, E. M. Kober and T. J. Meyer, *J. Phys. Chem.*, 1996, **100**, 2915.
- 12 N. Kitamura, M. Sato, H.-B. Kim, R. Obata and S. Tazuke, *Inorg. Chem.*, 1988, **27**, 651.
- 13 T. J. Meyer and P. Y. Chen, *Chem. Rev.*, 1998, **98**, 1439.
- 14 F. Barigelletti, A. Juris, V. Balzani, P. Belser and A. von Zelewsky, *Inorg. Chem.*, 1983, **22**, 3335.
- 15 A. Juris, V. Balzani, F. Barigelletti, S. Campagna, P. Belser and A. von Zelewsky, *Coord. Chem. Rev.*, 1988, **84**, 85.
- 16 X. Zhang, M. Kozik, N. Sutin and J. R. Winkler, *Adv. Chem. Ser.*, 1991, **228**, 245.
- 17 F. A. Cotton and G. Wilkinson, *Advanced Inorganic Chemistry*, Wiley, New York, 5th edn., 1988.
- 18 L. Sacksteder, M. Lee, J. N. Demas and B. A. DeGraff, *J. Am. Chem. Soc.*, 1993, **115**, 8230.
- 19 M. Sano, H. Kashiwagi and H. Yamatera, *Inorg. Chem.*, 1982, **21**, 3837.
- 20 E. M. Kober, J. V. Caspar, R. S. Lumpkin and T. J. Meyer, *Phys. Chem.*, 1986, **90**, 3722.
- 21 F. Barigelletti, A. Juris, V. Balzani, P. Belser and A. von Zelewsky, *J. Phys. Chem.*, 1987, **91**, 1095.
- 22 T. J. Meyer, *Pure Appl. Chem.*, 1986, **90**, 1193.
- 23 B. Durham, J. V. Caspar, J. K. Nagle and T. J. Meyer, *J. Am. Chem. Soc.*, 1982, **104**, 3803.
- 24 D. P. Rillema, C. B. Blanton, R. J. Shaver, D. C. Jackman, M. Boldaji, S. Bundy, L. A. Worl and T. J. Meyer, *Inorg. Chem.*, 1992, **31**, 1600; I. M. Barclay and J. A. Butler, *Trans. Faraday Soc.*, 1938, **34**, 1445.

Paper 9/05783H